Synthesis and structure of phases containing $[Ni_3P_3S_{12}]^{3-}$ crown-shaped trimers

Martine Bujoli-Doeuff,[a] Servane Coste,[a] Michel Evain,[a] Raymond Brec,[a] Dominique Massiot[b] and Stéphane Jobic*[a]

[a] *Laboratoire de Chimie des Solides, Institut des Matériaux Jean-Rouxel, (CNRS UMR 6502) 2 rue de la Houssinière, BP 32229, 44322 Nantes cedex 3, France. E-mail: joloic@cnrs-imn.fr; Fax: +33 2 40 37 39 95; Tel: +33 2 40 37 39 17*

[b] *Centre de Recherches sur la Physique des Hautes Températures, (CNRS UPR 4212), 1D Avenue de la Recherche Scientifique, 45071 Orléans cedex 02, France. E-mail: massiot@cnrs-orleans.fr*

Received (in Montpellier, France) 18th January 2002, Accepted 13th March 2002
First published as an Advance Article on the web

The exfoliation process of one-dimensional $KNiPS_4$ showed that the breaking of $^1/_\infty[NiPS_4]^-$ chains in polar solvent was followed by the formation of cyclic $[Ni_3P_3S_{12}]^{3-}$ trianions. From DMF–$KNiPS_4$ solutions, metathesis experiments were successfully carried out, but, up to now, K^+ had only been exchanged by bigger isotropic organic cations such as PPh_4^+, $(CH_3)_4N^+$ and $(C_2H_5)_4N^+$. After recrystallization, each metathesis compound presents the cyclic $[Ni_3P_3S_{12}]^{3-}$ trianion. An exchange by anisotropic cations is possible by adding a cryptand molecule that fits the size of K^+. Following this procedure, three new nickel thiophosphate complexes have been synthesized: $[Ni_3P_3S_{12}][K\text{-}(222\text{-cryptand})]_3$ (**I**), $[Ni_3P_3S_{12}][K(222\text{-cryptand})]_2[C_9N_1H_{22}]$ (**II**) and $[Ni_3P_3S_{12}][CH_3(CH_2)_{11}N(CH_3)_3]_3$ (**III**). The structures of **I** and **II** have been fully determined from single crystal X-ray diffraction analysis. They show the occurrence of the $[Ni_3P_3S_{12}]^{3-}$ trimer within the solid. **I** and **II** crystallize in the $P2_12_12_1$ space group. ^{31}P solid state NMR experiments hint at the presence of polyanions in **III**, maybe trianionic in nature.

The low-dimensional materials A_xMQ_y[1,2] (A = alkali metal, M = transition metal, lanthanide and/or main group element, Q = S, Se) exhibit structural arrangements that depend strongly upon the A/M ratio and the nature of the countercation.[3–5] To some extent, such compounds can be viewed as strongly covalently bonded, negatively charged domains electrostatically shielded from each other by alkali metal counterions. These alkali metals are only engaged in ionic bonds with the peripheral Q^{2-} chalcogenide anions of the covalent edifices. Thus, the structure can physically be split up into regions of covalent and ionic character. The higher the concentration and/or the larger the size of A,[6,7] the lower the dimensionality of the covalent sub-network. This phenomenon originates from the tendency of the system to maximize the attractive Coulombic interactions between alkali metal and chalcogen ions and to minimize the ionic repulsions between anions and between cations for a given alkali metal concentration.

Owing to the existence of covalent and ionic chemical links, A_xMQ_y materials can be considered, to some extent, as ionic $A_x^+[MQ_y]_x^-$ constructions that are expected to behave as salts in solutions. Hence, exfoliation and dissolution processes in polar organic solvents can be envisioned. On contact with a solvent, the inorganic solid may swell due to the diffusion of solvent molecules into the tridimensional inorganic edifice. As the A^+ cation is solvated, the A–Q distances increase and the electrostatic repulsions between the anionic covalent domains decline concomitantly. Then, a complete dispersion of the $A^+_x(sol)_z[MQ_y]^{x-}$ compound may happen, giving rise to colloïdal solutions containing layers, ribbons or discrete inorganic entities, depending on the structure of the A_xMQ_y solids. If the inorganic blocks are highly anisotropic, rigid enough and with colloïdal dimensions (10–1000 nm),[8] inorganic core based lyotropic nematic phases or liquid crystals may result. Depending on the solvent nature, the temperature and the concentration of the colloïdal particles, isotropic suspensions, nematic sols or/and nematic gels are expected to form.

Up to now, theoretical understanding of the exfoliation phenomenon is far from complete and the prediction of such reactions remains difficult. Usually, the exfoliation process is explained on the basis of a competition between the lattice energy and the solvation energy of the alkali metal and, to a lesser extent, of the anionic framework.[9] The chemical reaction is favored by the use of a solvent with a high ε dielectric constant and of small and highly polarizing countercations.[10] As a first approximation, the ε value of the solvent and the nature of the alkali metal in the A_xMQ_y compounds may serve as a guideline in judging whether or not a solid will dissolve. These factors have been highlighted in the pioneer work of Tarascon *et al.*[11] on exfoliation-dissolution in organic solvents of different members of the AMo_3Se_3 series (A = Li, Na, K). Considering the cation nature, it was observed that the Li derivative was easily soluble in *N*-methylformamide (NMF), the Na derivative partially soluble while KMo_3Se_3 was not soluble at all. This behavior agrees well with a decrease of the solvation energy of the alkali metal when its size increases. Likewise, $LiMo_3Se_3$ dissolves better in *N*-methylformamide ($\varepsilon = 182$) than in dimethylsulfoxide (DMSO, $\varepsilon = 46.7$) or in tetrahydrofuran (THF, $\varepsilon = 7.32$), in agreement with a decrease of the dielectric constant.

In fact, these criteria are not sufficient to account in full for the solvent–inorganic phase interaction, the solvating power of a solvent being a complex phenomenon related to additional factors such as the solvent basicity, its acidity and polarity and its self-association. Practically, it appears very difficult to

 DOI: 10.1039/b200703g

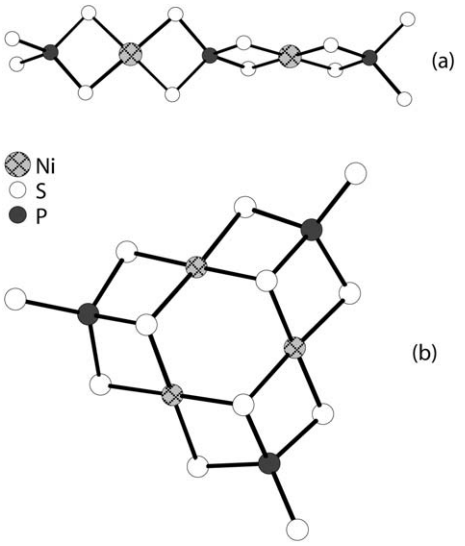

Fig. 1 (a) Linear fragment of the infinite $^1/_\infty[NiPS_4]^-$ chain of $KNiPS_4$ showing the $[NiS_4]$ squares sharing two edges with two $[PS_4]$ tetraedra. (b) Crown-shape of the discrete $[Ni_3P_3S_{12}]^{3-}$ oligomer present in the structures of $A_3[Ni_3P_3S_{12}]$ [$A = (Ph_4P)^+$, $(CH_3)_4N^+$, $(C_2H_5)_4N^+$, $(C_7H_{16}ON^+)$]. $[NiS_4]$ entities share two edges with two $[PS_4]$ tetraedra and two corners with two other $[NiS_4]$ squares.

predict *a priori* the reactivity of a solid on contact with a solvent, even for an isostructural series of materials.

Recently, some studies in solution have been carried out on $KNiPS_4$ and $KPdPS_4$. Both materials are isostructural and exhibit a 1D crystal structure associated with the existence of $^1/_\infty[MPS_4]^-$ infinite chains (M = Ni, Pd). The chains are built upon $[MS_4]$ squares and $[PS_4]$ tetraedra sharing edges [Fig. 1(a)].[12,13] Although both $KNiPS_4$ and $KPdPS_4$ exfoliate in DMF and DMSO, they exhibit different behavior in solution. While $^1/_\infty[PdPS_4]^-$ chains are maintained in solution leading to a complex fluid, $^1/_\infty[NiPS_4]^-$ chains undergo a solvent-induced auto-fragmentation with reorganization into discrete crown-shaped $[Ni_3P_3S_{12}]^{3-}$ oligomers [Fig. 1(b)]. In contrast to the $^1/_\infty[NiPS_4]^-$ chains, in the $[Ni_3P_3S_{12}]$ oligomer each $[NiS_4]$ entity shares two edges with two $[PS_4]$ tetraedra and two corners with two other $[NiS_4]$ squares. The breaking up of the chains into $[Ni_3P_3S_{12}]$ entities, corresponding to a shift from anisotropic to isotropic particles, was first evidenced by the loss of birefringence for the solution. The exfoliation and fragmentation of the chains in solution have been studied by mass spectroscopy and ^{31}P NMR of the sols.[14,15] So far, the mechanism of the cyclization and fragmentation of the chain, as the attack of the solvent at the atomic level on the inorganic solid, remains unknown.

Exchange reactions have been considered to take advantage of the formation of the anionic molecular $[Ni_3P_3S_{12}]^{3-}$ species in DMF solution. So far, potassium cations have been substituted by isotropic monovalent organic cations such as tetraphenyl phosphonium, tetramethyl ammonium and tetraethyl ammonium, and slightly anisotropic methyl morpholinium,[15] leading to $A_3[Ni_3P_3S_{12}]$ compounds with the stabilization, in the solid state, of crown-shaped $[Ni_3P_3S_{12}]^{3-}$ anions. Exchange with mono-charged, long alkyl chain cations has remained unsuccessful up to now.

In this paper we report a novel way of preparing new compounds by metathesis between K^+ and long chain *N*-alkylammonium cations with the help of a cryptand. The macrocyclic molecule, well known to selectively encapsulate cations of the appropriate size, should increase the solubility of $KNiPS_4$ in various polar solvents by complexing the cation and promoting the ion exchange reactions. The macrotricyclic molecule used in this work, 4,7,13,16,21,24-hexaoxa-1,10-diazobicyclo[8.8.8]hexacosane, symbolized by (222-cryptand),

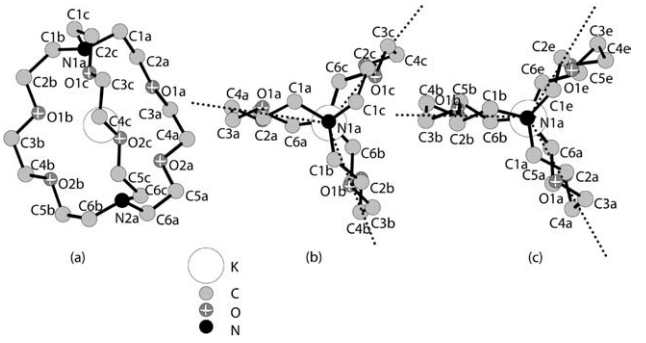

Fig. 2 (a) A cryptate entity with its cage and potassium inside. (b) View of the cryptate along its threefold axis in **I**. The $[C_6H_{12}O_2]$ fragments are symmetrically equivalent through a pseudo threefold axis running through N_1 and N_2. (c) Same view for **II**: one of the $[C_6H_{12}O_2]$ fragments is bent away from its symmetry plane. The other two $[C_6H_{12}O_2]$ fragments are symmetrically equivalent through a 120° rotation.

is very well suited for the complexation of potassium ions ($r_{K+} = 1.33$ Å) because of the adapted size of its cavity ($r = 1.4$ Å) [Fig. 2(a)].

In this article is reported the metathesis of $[Ni_3P_3S_{12}][K\text{-}(222\text{-cryptand})]_3$ (**I**), $[Ni_3P_3S_{12}][K(222\text{-cryptand})]_2[C_9N_1H_{22}]$ (**II**) and $[Ni_3P_3S_{12}][CH_3(CH_2)_{11}N(CH_3)_3]_3$ (**III**), the structure determination of **I** and **II** and the NMR analysis of **I** and **III**.

Experimental

Synthesis

All experiments and manipulations were performed under dry nitrogen using a Schlenk line. The organic chemicals were used as obtained. $KNiPS_4$ was prepared as previously described.[12]

$[Ni_3P_3S_{12}][K\text{-}(222\text{-cryptand})]_3$ (I). $KNiPS_4$ (190 mg, 0.74 mmol) was dissolved in 10 ml of DMF under magnetic stirring at 50 °C for 1 day. After filtration, 289.7 mg (0.77 mmol) of (222)-cryptand ($C_{18}O_6N_2H_{36}$, Aldrich, 98%) was added to the solution. After stirring for 1 h, the product was precipitated by adding diethyl ether. The precipitate was washed with ethanol and recrystallised by evaporation of dichloromethane under ambiant conditions. The obtained brown crystals are air-stable and soluble in DMF, acetonitrile, dichloromethane and chloroform but insoluble in pentane and diethyl ether. An EDXS (energy dispersive X-ray spectroscopy) analysis of the heaviest elements by means of a Jeol microscope (PGT-IMIX-PTS equipped Jeol-JSM5800LV) yielded the elemental ratio $Ni_{3.0} : P_{3.0} : S_{13.5} : K_{2.7}$, in fair agreement with the X-ray determined composition $[Ni_3P_3S_{12}][K_1\text{-}(222\text{-cryptand})]_3$.

$[Ni_3P_3S_{12}][K(222\text{-cryptand})]_2[C_9N_1H_{22}]$ (II). The metathesis was similar to that of **I**, except that 201.76 mg (0.9 mmol) of *n*-hexyltrimethylammonium bromide (Interchim) was poured into the $KNiPS_4$–DMF solution in addition to the cryptand. After stirring of the solution for 2 h, diethyl ether was added and the product was washed with ethanol and acetone. Air-stable crystals suitable for X-ray structure determination could be obtained by slow evaporation of a dichloromethane solution. Several brown crystals were analyzed by EDXS. The heavy element mean composition was $Ni_{2.7} : P_{3.0} : S_{12.3} : K_{1.5} : N_{3.9}$ in accord with the formula $[Ni_3P_3S_{12}]K_2[C_{45}N_5O_{12}H_{94}]$.

$[Ni_3P_3S_{12}][CH_3(CH_2)_{11}N(CH_3)_3]_3$ (III). The metathesis was analogous to that of **I**, except that 277.5 mg (0.9 mmol) of dodecyltrimethylammonium bromide (Aldrich, 99%) was

added in addition to the cryptand. The analysis of the heavy elements of the crystals by EDXS yielded the formula $Ni_{3.0} : P_{3.0} : S_{11.1} : N_{4.2}$, corresponding to the expected $[Ni_3P_3S_{12}][C_{45}H_{104}N_3]$ formula. Note that without cryptand, the cationic exchange fails. Unfortunately, the crystal quality was too poor for any X-ray structural investigation.

X-Ray crystallographic studies

For data collection, a crystal of **I** and **II** was glued with nail polish at the tip of a Lindemann quartz glass capillary. Reflection intensities were then collected at 120 K for **I** and 150 K for **II** on a Stoe imaging plate diffraction system, which was configured in a medium resolution mode (IP at 100 mm limiting $\sin(\theta)/\lambda$ to 0.50 $Å^{-1}$ for **I** and 80 mm limiting $\sin(\theta)/\lambda$ to 0.51 $Å^{-1}$ for **II**). The reflections were first corrected for the Lorentz polarization with the STOE IPDS software package.[16] The structures were then solved by means of SHELXS direct methods[17] in the $P2_12_12_1$ space group. All supplementary treatments and calculations were carried out with the JANA2000 software package.[18] Data collection parameters, refinement conditions and results for **I** and **II** are summarized in Table 1.

CCDC reference numbers 185895 and 185896. See http://www.rsc.org/suppdata/nj/b2/b200703g/ for crystallographic data in CIF or other electronic format.

$[Ni_3P_3S_{12}][K\text{-}(222\text{-cryptand})]_3$ (I). The 29734 reflections were merged according to the 222 point group, yielding 9004 independent reflections, of which 3650 with $I > 2\sigma(I)$ were retrieved. Taking into account all of the unconstrained atoms of the cryptand molecule did not lead to satisfactory refinement. Because of the great number of parameters and of the symmetry of the cryptand molecule (quasi-threefold axis through the two nitrogen atoms) [Fig. 2(b)], the "rigid body" option of JANA2000 was used. The three $[C_6H_{12}O_2]$ fragments constituting the cryptant molecule ($C_{18}H_{36}O_6N_2$) were considered to be identical to each other. The atomic positions of a fragment [from C_1 to C_6, Fig. 2(a)] were refined, the others being deduced through 120° rotations. Finally, the H atoms of the $[CH_2]$ groups were added so that the C–H distances were equal to 1.0 Å, their coordinates were fixed and all the isotropic displacement parameters (IDP's) were set to 0.121(9) $Å^2$. The reliability factor then converged to $R_{F^2}(obs)/R_{wF^2}(obs) = 0.0852/0.1467$ (368 parameters and 3650 reflections) with a featureless difference Fourier maps.

Table 1 Crystal, X-ray data collection, and refinement parameters for **I** and **II**

	I	**II**
Chemical formula	$[Ni_3P_3S_{12}]$ $[K\text{-}(222\text{-cryptand})]_3$	$[Ni_3P_3S_{12}]$ $[K(222\text{-cryptand})]_2$ $[C_9N_1H_{22}]$
Molecular weight	1900.49	1629.18
Crystal system	Orthorhombic	Orthorhombic
Space group	$P2_12_12_1$	$P2_12_12_1$
a/Å	16.4431(10)	18.296(2)
b/Å	22.1019(11)	29.174(2)
c/Å	24.1758(14)	13.5323(14)
U/$Å^3$	8786.1(9)	7222.9(12)
Z	4	4
μ/mm^{-1}	1.178	1.356
T/K	120	150
Total reflections	29734	57092
Independent reflections	9004	10801
Observed reflections $[I > 2\sigma(I)]$	3650	5030
R_{int} (obs)	0.07	0.09
R (obs)[a]	0.0852	0.0511
R_w (obs)[a]	0.1467	0.0836
R (all)[a]	0.1837	0.1321
R_w (all)[a]	0.1658	0.1049
Weighting scheme		

[a] $R = \Sigma||F_o|-|F_c||/\Sigma|F_o|$ and $wR_{F^2} = [\Sigma w_{F^2}(|F_o|^2-|F_c|^2)^2/\Sigma w_{F^2}|F_o|^4]^{1/2}$ where $w_{F^2} = 1/[\sigma^2(I_0) + (0.001024 \times I_0)^2]$.

$[Ni_3P_3S_{12}][K(222\text{-cryptand})]_2[C_9N_1H_{22}]$ (II). The reflection set was first merged according to the 222 point group, yielding 10801 independent reflections, of which 5030 with $I > 2\sigma(I)$ were retrieved. A rigid body model set up for the refinement of **I** was once again used to reduce the number of parameters. However, in this case, the refinement was not satisfactory. Actually, as was found later, the cryptand molecule had lost its pseudo threefold symmetry axis. In fact, among the three $[C_6H_{12}O_2]$ fragments, two were still related by a pseudo 120° rotation whereas the third was not, due to its distortion [Fig. 2(c)]. Thus, the two first $[C_6H_{12}O_2]$ groups were refined using the rigid body constraint whereas the atoms of the third group were refined independently. In addition, the O–C and the K–O distances in the non-symmetric fragment were soft restrained to vary in the 1.42–1.48 Å and 2.67–2.73 Å ranges, respectively. Finally, the H atoms of the $[CH_2]$ groups were added by fixing their coordinates and their IDPs to 0.095(5) $Å^2$. The refinement was completed by applying a type 1 lorentzian extinction coefficient.[19] The reliability factor converged then to $R_{F^2}(obs)/R_{wF^2}(obs) = 0.0511/0.0836$ (546 parameters and 5030 reflections) with featureless difference Fourier maps.

NMR spectroscopy

Solid state ^{31}P NMR spectra were recorded on a Bruker DSX400 spectrometer operating at 9.4 T, using CP-MAS $\{^1H\}$-^{31}P excitation with a typical contact time of 1.5 ms and 1 s recycle time. Spectra were simulated using the "dmfit" software package.[20]

Results and discussion

Structure description

$[Ni_3P_3S_{12}][K\text{-}(222\text{-cryptand})]_3$ (I). The unit cell of **I** contains four equivalent $[Ni_3P_3S_{12}]^{3-}$ motifs. Their structural arrangement turns out to be the same as the one previously described in the series of $A_3[Ni_3P_3S_{12}]$ [$A = (Ph_4P)^+$, $(CH_3)_4N^+$, $(C_2H_5)_4N^+$, $(C_7H_{16}ON^+)$][14] compounds. The $[Ni_3P_3S_{12}]^{3-}$ anions can be described as a bowl-like structure having a pseudo threefold symmetry axis (even though the three metal and phosphorus sites of each trimer are crystallographically inequivalent, they are chemically identical). It can be noticed that, in all these structures, the P^{V}–S^{-II} and Ni^{II}–S^{-II} distances are in good agreement with the sum of the ionic radii.[21]

The cryptand molecule has a pseudo/threefold axis, going through the two nitrogen atoms, so that the $[O_2C_6H_{12}]$ fragments can be considered as equivalent, as explained before [Fig. 2(b)]. The potassium cations, found indeed encapsulated in the cryptand cage, are bound to six oxygen atoms with K–O distances ranging from 2.75 to 2.88 Å and to two nitrogen atoms with K–N distances ranging from 2.90 to 3.02 Å.

The 3D arrangement of **I** (Fig. 3) can be described as an alternate stacking of $[Ni_3P_3S_{12}]^{3-}$ anions and $[K\text{-}(222\text{-cryptand})]^+$ layers along the [010] axis. The thiophosphate layers are built upon head-to-foot crown-shaped $[Ni_3P_3S_{12}]^{3-}$ trimers. The pseudo threefold axes of the $[Ni_3P_3S_{12}]^{3-}$ and (222-cryptand) groups are almost perpendicular to these layers. Note that both $KNiPS_4$ and $[K\text{-}(222\text{-cryptand})]NiPS_4$ structures containing $^1/_\infty[NiPS_4]^-$ chains and $[Ni_3P_3S_{12}]^{3-}$ anions, respectively, can be described as resulting from the

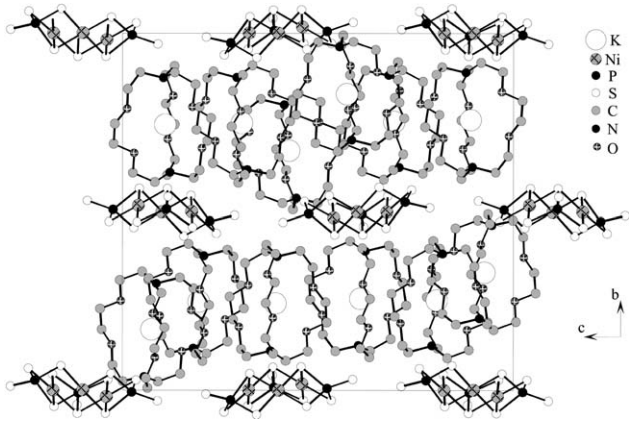

Fig. 3 View along the *a* axis of $[Ni_3P_3S_{12}][K\text{-}(222\text{-cryptand})]_3$ (**I**). This compound can be described as $^2/_\infty[NiPS_4]^-$ layers of discrete $[Ni_3P_3S_{12}]^{3-}$ entities separated by layers of cryptate molecules, K-(222-cryptand)$^+$, corresponding to a 2D arrangement. H atoms are not been represented.

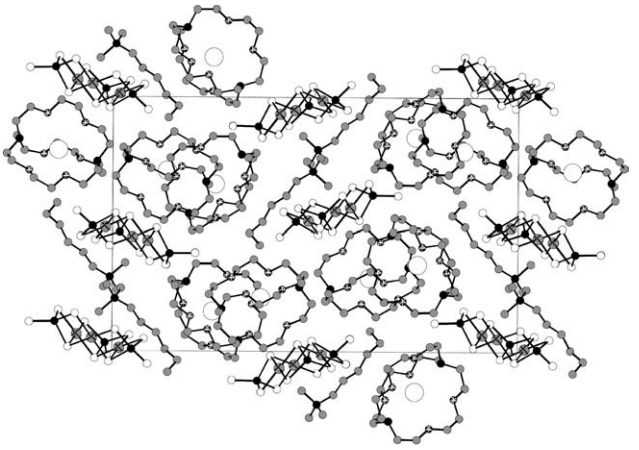

Fig. 4 View along the *c* axis of $[Ni_3P_3S_{12}][K(222\text{-cryptand})]_2[C_9N_1H_{22}]$ (**II**). Because of the stacking along the *c* axis of the discrete $[Ni_3P_3S_{12}]^{3-}$ entities and of the cryptates and N-alkyl ammonium molecules, the arrangement is 1D.

stacking of $^2/_\infty[K^+]$ and $^2/_\infty[NiPS_4]^-$ layers. Let us emphasize that the lowering of the dimensionality of the covalent network when going from $KNiPS_4$ to $[K\text{-}(222\text{-cryptand})]NiPS_4$ agrees well, as expected, with the increase of the size of the countercation ($r_{K^+} = 1.33$ Å and $r_{K(222-cryptand)^+} = 3.7$ Å).

The main distances and angles in $[Ni_3P_3S_{12}]^{3-}$ are reported in Table 2 whereas, for the 222-cryptand, they are given in the ESI.

$[Ni_3P_3S_{12}][K(222\text{-cryptand})]_2[C_9N_1H_{22}]$ (II). The unit cell is composed of four equivalent discrete $[Ni_3P_3S_{12}]^{3-}$ anions, four equivalent hexyltrimethylammonium $[CH_3(CH_2)_5N(CH_3)_3]^+$ cations and eight cryptand molecules with potassium cations inside (Fig. 4). The $[Ni_3P_3S_{12}]^{3-}$ anions are the same as in **I**. The main distances and angles in the trimer are reported in Table 2. The hexyltrimethylammonium groups can be described as zigzag chains (length ~7.7 Å) with the terminal methyl

Table 2 Main distances (Å) and angles (°) and corresponding esd's in the $[Ni_3P_3S_{12}]^{3-}$ anion for **I** and **II**

NiS_4 sites				*PS_4 sites*			
I							
Ni(1)–S(1)	2.204(8)	S(1)–Ni(1)–S(4)	87.7(3)	P(1)–S(1)	2.188(9)	S(1)–P(1)–S(5)	92.4(3)
Ni(1)–S(9)	2.198(7)	S(1)–Ni(1)–S(3)	93.5(3)	P(1)–S(5)	2.053(9)	S(1)–P(1)–S(10)	125.4(5)
Ni(1)–S(4)	2.204(6)	S(9)–Ni(1)–S(4)	91.0(2)	P(1)–S(10)	1.887(8)	S(1)–P(1)–S(4)	92.0(3)
Ni(1)–S(3)	2.208(7)	S(9)–Ni(1)–S(3)	87.9(2)	P(1)–S(4)	2.055(8)	S(5)–P(1)–S(10)	114.5(3)
Ni(2)–S(1)	2.225(7)	S(1)–Ni(2)–S(5)	87.3(3)	P(2)–S(6)	2.054(9)	S(5)–P(1)–S(4)	113.8(3)
Ni(2)–S(6)	2.220(6)	S(1)–Ni(2)–S(2)	94.2(3)	P(2)–S(2)	2.097(8)	S(10)–P(1)–S(4)	115.6(4)
Ni(2)–S(5)	2.212(7)	S(2)–Ni(2)–S(6)	86.5(2)	P(2)–S(11)	1.944(8)	S(6)–P(2)–S(2)	94.0(3)
Ni(2)–S(2)	2.210(7)	S(5)–Ni(2)–S(6)	92.0(2)	P(2)–S(7)	2.044(9)	S(6)–P(2)–S(11)	114.6(4)
Ni(3)–S(2)	2.233(7)	S(2)–Ni(3)–S(7)	87.4(2)	P(3)–S(12)	1.931(8)	S(6)–P(2)–S(7)	114.1(4)
Ni(3)–S(7)	2.227(7)	S(2)–Ni(3)–S(3)	92.3(2)	P(3)–S(9)	2.060(8)	S(2)–P(2)–S(11)	120.0(5)
Ni(3)–S(8)	2.214(7)	S(7)–Ni(3)–S(8)	93.2(3)	P(3)–S(8)	2.044(9)	S(2)–P(2)–S(7)	96.1(3)
Ni(3)–S(3)	2.210(7)	S(8)–Ni(3)–S(3)	87.1(3)	P(3)–S(3)	2.136(9)	S(11)–P(2)–S(7)	115.2(4)
Ni–S	2.214			P–S	2.041	S(12)–P(3)–S(9)	115.2(3)
						S(12)–P(3)–S(8)	116.7(3)
						S(12)–P(3)–S(3)	119.8(5)
						S(9)–P(3)–S(8)	113.6(4)
						S(9)–P(3)–S(3)	93.6(3)
						S(8)–P(3)–S(3)	93.6(3)
II							
Ni(1)–S(1)	2.217(2)	S(1)–Ni(1)–S(3)	91.59(10)	P(1)–S(1)	2.106(3)	S(1)–P(1)– S(4)	94.69(16)
Ni(1)–S(3)	2.209(2)	S(1)–Ni(1)–S(4)	87.21(11)	P(1)–S(4)	2.061(4)	S(1)–P(1)–S(5)	94.94(16)
Ni(1)–S(4)	2.226(3)	S(3)–Ni(1)–S(9)	87.32(11)	P(1)–S(5)	2.048(4)	S(1)–P(1)–S(10)	118.97(16)
Ni(1)–S(9)	2.221(2)	S(4)–Ni(1)–S(9)	93.88(11)	P(1)–S(10)	1.937(3)	S(4)–P(1)–S(5)	112.18(16)
Ni(2)–S(1)	2.206(3)	S(1)–Ni(2)–S(2)	91.43(11)	P(2)–S(2)	2.128(4)	S(4)–P(1)–S(10)	116.23(19)
Ni(2)–S(2)	2.215(2)	S(1)–Ni(2)–S(5)	87.79(11)	P(2)–S(6)	2.066(4)	S(5)–P(1)–S(10)	116.2(2)
Ni(2)–S(5)	2.209(3)	S(2)–Ni(2)–S(6)	88.46(11)	P(2)–S(7)	2.045(4)	S(2)–P(2)–S(6)	94.88(16)
Ni(2)–S(6)	2.214(3)	S(5)–Ni(2)–S(6)	92.24(12)	P(2)–S(11)	1.944(4)	S(2)–P(2)–S(7)	93.52(18)
Ni(3)–S(2)	2.207(2)	S(2)–Ni(3)–S(3)	92.50(11)	P(3)–S(3)	2.115(3)	S(2)–P(2)–S(11)	119.04(17)
Ni(3)–S(3)	2.218(3)	S(2)–Ni(3)–S(7)	87.21(12)	P(3)–S(8)	2.052(4)	S(6)–P(2)–S(7)	111.87(16)
Ni(3)–S(7)	2.203(3)	S(3)–Ni(3)–S(8)	87.56(12)	P(3)–S(9)	2.056(4)	S(6)–P(2)–S(11)	116.0(2)
Ni(3)–S(8)	2.205(3)	S(7)–Ni(3)–S(8)	92.78(12)	P(3)–S(12)	1.951(4)	S(7)–P(2)–S(11)	117.52(19)
Ni–S	2.212			P–S	2.042	S(3)–P(3)–S(8)	94.50(17)
						S(3)–P(3)–S(9)	94.34(16)
						S(3)–P(3)–S(12)	118.88(17)
						S(8)–P(3)–S(9)	112.95(18)
						S(8)–P(3)–S(12)	116.3(2)
						S(9)–P(3)–S(12)	116.1(2)

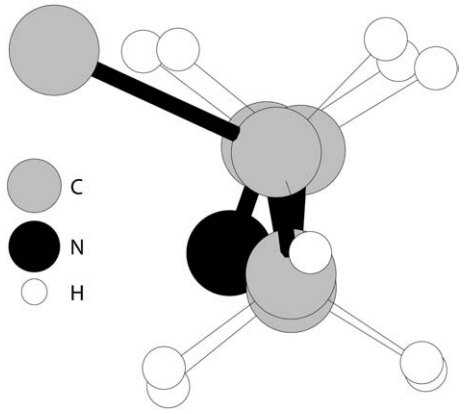

Fig. 5 View along the alkyl chain of the hexyltrimethylammonium groups. The carbon of the terminal methyl is strongly shifted from the plane defined by the nitrogen and the carbons of the chain. The methyl groups linked to the N atom have been removed for clarity.

group of the alkyl chain strongly shifted from the plane formed by the other carbon atoms (Fig. 5) because of a neighbouring cryptand molecule. In this structure, the cryptates do not keep their pseudo threefold axis as in **I** [Fig. 2(c)], so that one of the $[C_6H_{12}O_2]$ fragments is dissymmetric in comparison with the other two.

At this stage, we may also notice that the arrangement of the $[Ni_3P_3S_{12}]^{3-}$ anions in tridimensional space depends upon the size and the shape of the organic countercations: going from $[K\text{-}(222\text{-cryptand})]_3Ni_3P_3S_{12}$ to $[K(222\text{-cryptand})]_2[C_9N_1H_{22}]\text{-}Ni_3P_3S_{12}$ and to $[PPh_4]_3Ni_3P_3S_{12}$, the relative arrangement of the discrete $[Ni_3P_3S_{12}]^{3-}$ trimers shifts from 2D to 1D to 0D.

NMR spectroscopy

Owing to the poor quality of the $[Ni_3P_3S_{12}][CH_3(CH_2)_{11}\text{-}N(CH_3)_3]_3$ (**III**) crystals, ^{31}P experiments were carried out on the powder to determine the presence of $[Ni_3P_3S_{12}]^{3-}$ oligomers. ^{31}P NMR spectra of $KNiPS_4$, $(PPh_4)_3[Ni_3P_3S_{12}]$ and **I** were used as references (Fig. 6). From previous work,[14,15] it is known that the ^{31}P solid state NMR spectrum of $KNiPS_4$ exhibits only one resonance at $\delta = 122$ ppm characteristic of the phosphorus in the chain, whereas that of $(PPh_4)_3[Ni_3P_3S_{12}]$ exhibits three resonances (in addition to those of the tetraphenylphosphonium group at $\delta = 23.8$ and 21.3 ppm) at 112.6, 109.6 and 106.4 ppm. These three resonances were assigned to the three crystallographically inequivalent P sites in the $[Ni_3P_3S_{12}]^{3-}$ anions and turned out to be very similar in intensity.

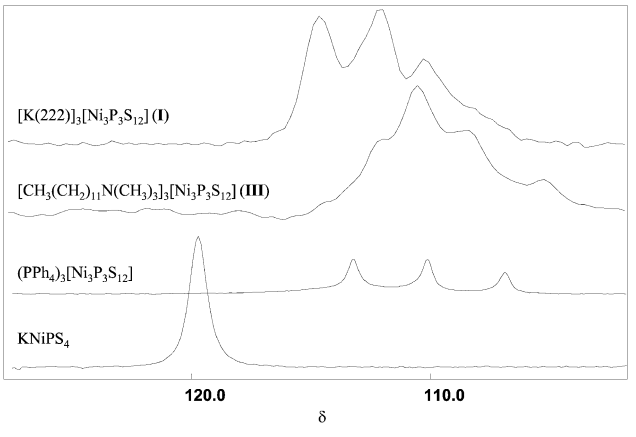

Fig. 6 Superposition of the $KNiPS_4$, $(PPh_4)_3Ni_3P_3S_{12}$, $[Ni_3P_3S_{12}]\text{-}[K\text{-}(222\text{-cryptand})]_3$ (**I**) and $[Ni_3P_3S_{12}][CH_3(CH_2)_{11}N(CH_3)_3]_3$ (**III**) ^{31}P solid state NMR spectra. The $KNiPS_4$ spectrum presents one peak at 122 ppm corresponding to the phosphorus inside the chain. $(PPh_4)_3Ni_3P_3S_{12}$ presents three peaks corresponding to the three phosphorus of $[Ni_3P_3S_{12}]^{3-}$. The two other spectra present also three peaks indicative of the presence of $[Ni_3P_3S_{12}]^{3-}$ trianion in **I** (as proven by the crystal structure) and also in **III**.

For **I**, the spectrum agrees well with the presence of the cyclic $[Ni_3P_3S_{12}]^{3-}$anion, as expected from the structural determination (see above). Three peaks are observed at 114.6, 112.2 and 109.9 ppm, that is at slightly higher δ values compared to $(PPh_4)_3[Ni_3P_3S_{12}]$. In addition, let us notice that a fourth peak shows up as a shoulder around 109 ppm.

The ^{31}P solid state NMR spectrum of **III** exhibits four peaks at 111.5, 110.5, 108.0 and 105.3 ppm. The first three, constituting a massif, may suggest the existence of trimeric entities in this material even if the relative intensities of the peaks are difference from those of $(PPh_4)_3[Ni_3P_3S_{12}]$. The fourth peak, which recalls the shoulder observed in **I**, is of unknown origin. Supplementary experiments are in progress to try to recrystallised the phase and to isolate the NMR trimer contribution for proper assignment of the resonances.

Concluding remarks

Our goal to synthesise a new $[Ni_3P_3S_{12}]^{3-}$ trimer in compounds containing anisotropic countercations has been successfully achieved. The exchange of an isotropic K^+ cation by an anisotropic cation has only been possible thanks to the adding of a cryptand molecule in the $KNiPS_4/ABr$ (A = anisotropic cation) DMF solution. X-ray diffraction analyses have showed for the well crystallised phase that they all contained the same $[Ni_3P_3S_{12}]^{3-}$ crown-shaped trimer. In the case of the amorphous material **III**, ^{31}P solid state NMR experiments hint at the presence of polyanions, perhaps trianionic in nature.

References

1 M. G. Kanatzidis and A. C. Sutorik, *Prog. Inorg. Chem.*, 1995, **43**, 151.
2 M. G. Kanatzidis, *Curr. Opin. Solid State Mater. Sci.*, 1997, **2**, 139.
3 W. Bronger and P. Müller, *J. Less Common Met.*, 1984, **100**, 241.
4 S.-P. Huang and M. Kanatzidis, *Inorg. Chem.*, 1991, **30**, 1455.
5 Y.-J. Lu and J. A. Ibers, *Comments Inorg. Chem.*, 1993, **14**, 229.
6 M. G. Kanatzidis, *Chem. Mater.*, 1990, **2**, 353.
7 S. Coste, E. Kopnin, M. Evain, S. Jobic, C. Payen and R. Brec, *J. Solid State Chem.*, 2001, **162**, 195.
8 J.-C. P. Gabriel and P. Davidson, *Adv. Mater.*, 2000, **12**, 9.
9 J. Rouxel, *Adv. Synth. React. Solids*, 1994, **2**, 27.
10 R. Dronskowski and R. Hoffmann, *Inorg. Chem.*, 1992, **31**, 3107.
11 J. M. Tarascon, F. J. Disalvo, C. H. Chen, P. J. Carroll, M. Walsh and L. Rupp, *J. Solid State Chem.*, 1985, **58**, 290.
12 S. H. Elder, A. Van der Lee, R. Brec and E. Canadell, *J. Solid State Chem.*, 1995, **116**, 107.
13 K. Chondroudis, M. G. Kanatzidis, J. Sayettat, S. Jobic and R. Brec, *Inorg. Chem.*, 1997, **36**, 5859.
14 J. Sayettat, L. M. Bull, S. Jobic, J.-C. P. Gabriel, M. Fourmigué, P. Batail, R. Brec, R.-L. Inglebert and C. Sourisseau, *J. Mater. Chem.*, 1999, **9**, 143.
15 J. Sayettat, L. M. Bull, J.-C. P. Gabriel, S. Jobic, F. Camerel, A.-M. Marie, M. Fourmigué, P. Batail, R. Brec and R.-L. Inglebert, *Angew. Chem., Int. Ed.*, 1998, **37**, 1711.
16 Stoe IPDS software, STOE & Cie GmbH, Darmstadt, Germany, 1996.
17 G. M. Sheldrick, SHELXTL, v. 5, Siemens Analytical X-Ray Instruments, Inc., Madison, WI, 1995.
18 V. Petricek and M. Dusek, JANA2000, Institute of Physics, Academy of Sciences of the Czech Republic, Prague, Czech Republic, 1998.
19 P. J. Becker and P. Coppens, *Acta Crystallogr., Sect. A*, 1974, **30**, 129.
20 D. Massiot, F. Favon, M. Capron, I. King, S. Le Calvé, B. Alonso, J-O. Durant, B. Bujoli, Z. Gan and G. Hoatson, *Magn. Res. Chem.*, 2002, **40**, 70.
21 R. D. Shannon in *Structure and Bonding in Crystals*, eds. M. O'keeffe and A. Navrotsky, Academic Press, New York, 1981, vol. 2, p. 61.